Full Paper

Design and Synthesis of Aza-Flavones as a New Class of Xanthine Oxidase Inhibitors

Rajni Dhiman[1], Sahil Sharma[1], Gagandip Singh[2], Kunal Nepali[1], and Preet Mohinder Singh Bedi[1]

[1] Department of Pharmaceutical Sciences, Guru Nanak Dev University, Amritsar, Punjab, India
[2] Laboratory of Drug Design, Department of Pharmaceutical Chemistry, ISF College of Pharmacy, Moga, Punjab, India

In an attempt to develop non-purine-based xanthine oxidase (XO) inhibitors, keeping in view the complications reported with the use of purine-based XO inhibitors, the flavone framework (a class possessing XO inhibitory potential) was used as lead structure for further optimization. By means of structure-based classical bioisosterism, quinolone was used as an isoster for chromone (a bicyclic unit present in flavones), owing to the bioactive potential and drug-like properties of quinolones. This type of replacement does not alter the shape and structural features required for XO inhibition, and also provides some additional interaction sites, without the loss of hydrogen bonding and hydrophobic and arene–arene interactions. In the present study, a series of 2-aryl/heteroaryl-4-quinolones (aza analogs of flavones) was rationally designed, synthesized and evaluated for *in vitro* XO inhibitory activity. Some notions about structure–activity relationships are presented indicating the influence of the nature of the 2-aryl ring on the inhibitory activity. Important interactions of the most active compound **3l** (IC_{50} = 6.24 μM) with the amino acid residues of the active site of XO were figured out by molecular modeling.

Keywords: Bioisosterism / Flavones / Isosteric / Quinolones / Xanthine oxidase

Received: July 24, 2012; Revised: August 29, 2012; Accepted: August 31, 2012

DOI 10.1002/ardp.201200296

Supporting information available online

Introduction

Xanthine oxidase (XO) is a versatile molybdoflavoprotein, widely distributed, occurring in milk, kidney, lung, heart, and vascular endothelium. In humans, the highest specific activity for XO is found in the liver and intestine. The enzyme is involved in the metabolism of purines, catalyzing the oxidative hydroxylation of hypoxanthine and xanthine to produce uric acid and reduction of oxygen at the flavin center generating reactive oxygen species either as superoxide anion radical or hydrogen peroxide (Fig. 1) [1–3]. Catalysis by XO to produce uric acid and reactive oxygen species leads to many diseases like gout and at least symptoms of diseases like oxidative damage to the tissue [2]. Involvement of reactive oxygen species in pathological events including inflammation, metabolic disorders, cellular ageing, atherosclerosis, and carcinogenesis is well reported [2, 3]. Increased XO serum level in pathological states like hepatitis, inflammation, cancer, etc. indicates that XO inhibition may result in broad spectrum therapeutics for gout, cancer, inflammation, and oxidative damage [2–5]. Despite the potential of purine based compounds as xanthine oxidative inhibitors such as allopurinol [3, 4], 2-alkyl hypoxanthines [6], pterin, and 6- formylpterin [7], there is a continuous search for non-purine based XO inhibitors. The revived interest among the researchers toward the XO inhibitors with structurally diverse and non-purine isosters [8] such as feboxustat [9], flavones [10], FYX, a 1,3-diaryltriazole [11] derivative, and curcumin [12] (Fig. 2) can be attributed to the interactions of purine analogs XO inhibitors on activities of purine and pyrimidine metabolizing enzymes like guanine deaminase, HGPRT (hypoxanthine–guanine phosphoribosyl transferase), PNP (purine nucleoside phosphorylase), OPRT (orotate phospho-ribosyl transferase) and OMPDC (orotidine-5-monophosphate decarboxylase) leading to Steven Johnson syndrome

Correspondence: Dr. Kunal Nepali, Department of Pharmaceutical Sciences, Guru Nanak Dev University, Amritsar-143005, Punjab, India.
E-mail: kunal_8855@rediffmail.com
Fax: +91-1832258819

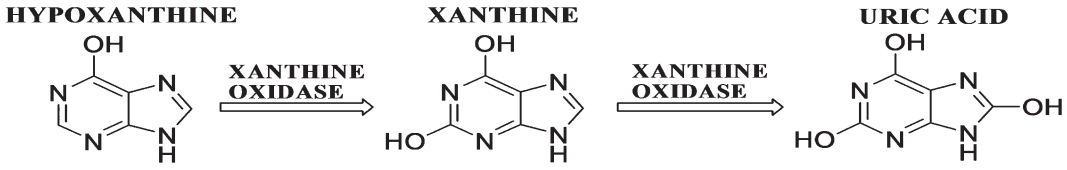

Figure 1. Role of XO.

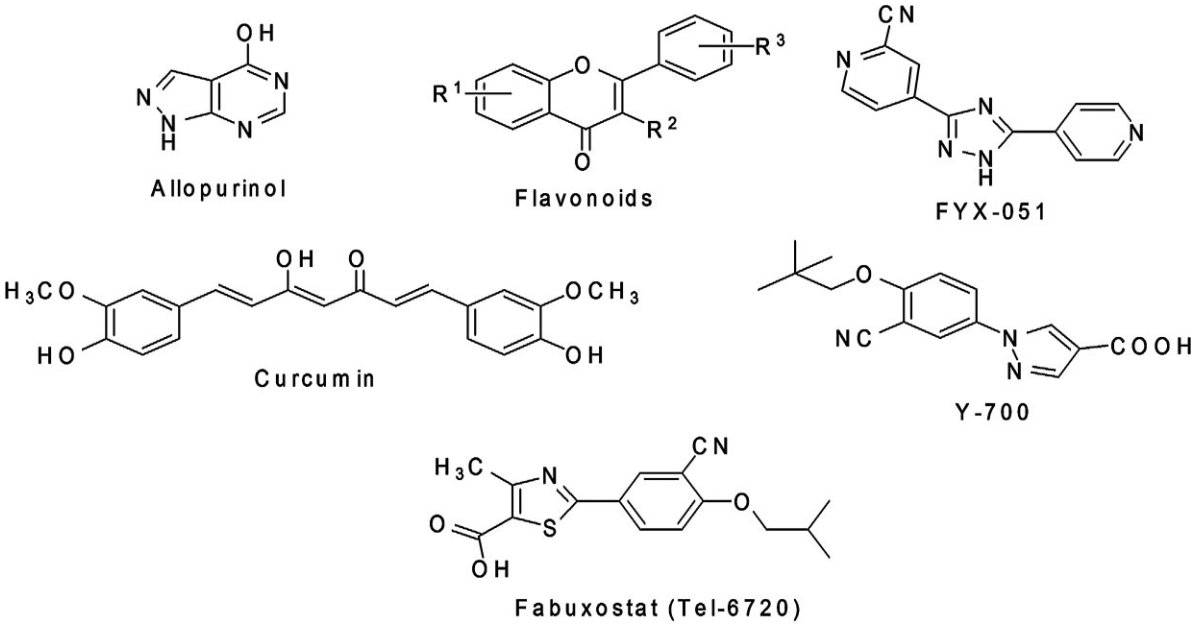

Figure 2. Some XO inhibitors.

and worsening of renal function induced in some of the patients [2–4].

Recently our research group reported the XO inhibitory potential of *N*-acetyl pyrazolines and *N*-(1,3-diaryl-3-oxo-propyl) [13, 14] amides designed via chemical modification of 1,3-diaryl triazoles (Fig. 3). In continuation of our search for non-purine based XO inhibitors, the present study utilizes the concept of classical bioisosterism employing 2-phenyl-chromone (flavone framework) as the lead structure.

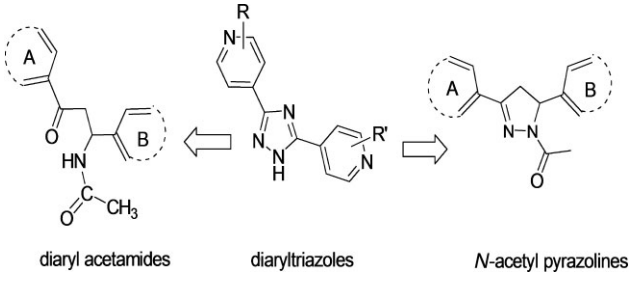

Figure 3. Chemical modification of 1,3-diaryl triazoles.

Bioisosterism, a lead optimization technique to enhance the biological activity or to attenuate the toxicity has proved to be an effective methodology to create therapeutically equivalent surrogates [15–18]. Flavonoids represent a class of secondary metabolites possessing a diverse array of biological activities such as anti-inflammatory [19], antiallergic [19, 20], antioxidant [20], CNS [21], vascular [22], antitumor [22], and XO inhibitors [23–25]. This family of secondary metabolites possesses a diverse array of biological activities but numerous reports on the XO inhibitory potential of flavones particularly highlights their potential as XO inhibitors. The structures of flavones with potent XO inhibitory activity are shown in Fig. 4. The pharmacophoric features responsible for XO inhibition by this class of secondary metabolites possessing the bicyclic benzopyrone as a core structural unit is well reported [23–25]. The rational design of 2-aryl-4-quinolones involving the isosteric replacement of chromones with quinolones (two being isoelectric analogues of one another) was thought worthwhile, keeping in view the shape and structural features of flavones responsible for their inhibitory potential (Fig. 5).

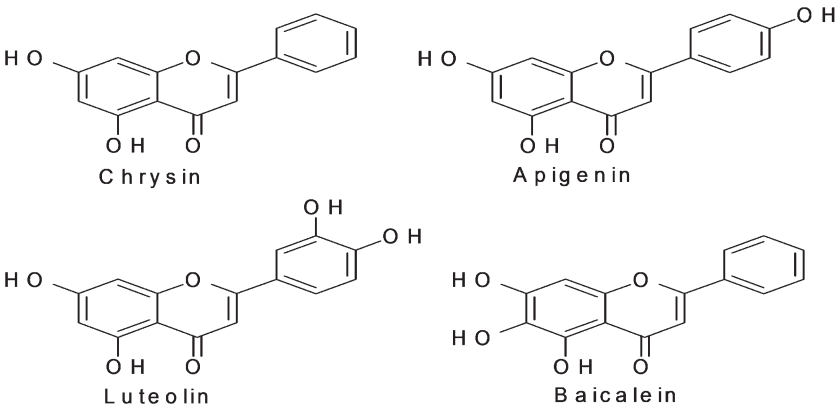

Figure 4. Flavones with XO inhibitory activity.

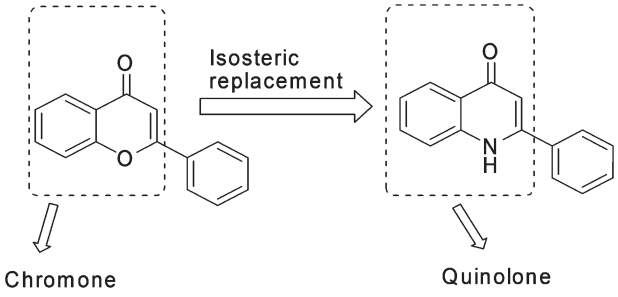

Figure 5. Isosteric replacement of the chromone nucleus with quinolone.

Quinolones as privileged building blocks allow the production of large libraries of bioactive molecules owing to their diversity and drug like properties and are considered as central scaffolds to build promising bioactive chemical libraries [26].

With this background, 2-aryl/heteroaryl-4-quinolones have been designed incorporating the quinolone nucleus within the chemical architecture of flavones based on the considerations earlier reported to be essential for the XO inhibitory activity of flavones [23–25] (Fig. 6) such as: (i) a bicyclic nucleus appropriate for hydrophobic and arene–arene interaction; (ii) an olefinic center at C-2,3 maintaining the planarity of the designed molecules; (iii) an appropriately placed carbonyl function for hydrogen bonding interaction; (iv) an appropriately placed aryl/heteroaryl ring for hydrophobic interactions; (v) an appropriate torsional angle; (vi) a substituent free C-3 center earlier reported to lower the binding affinity of flavones [23–25]. As the designed molecules are derived from non-purine based skeletons, it also excludes the possibility of them being converted like allopurinol to natural nucleotides.

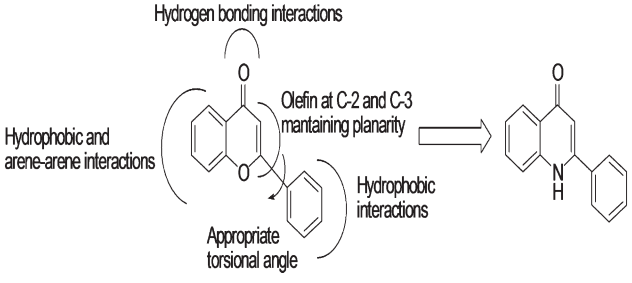

Figure 6. Key Interactions and structural features.

In the present paper, we describe the synthesis of non-purine 2-aryl/heteroaryl-4-quinolones without ignoring shape and structural features as a new class of XO inhibitors for the first time. The results of the biological evaluation have been further rationalized by the aid of computational studies.

Results and discussion

Chemistry

2-Aryl-4-quinolones were synthesized (Scheme 1) via a sequence of reactions starting from 2-amino benzoic acid which was converted to 2-aminoacetophenone employing methyl lithium in dimethyl ether. The 2-amino acetophenone was further acetylated to prevent any imine formation on condensation with different substituted aldehydes. All the diaryl propenones were synthesized by base catalyzed Claisen Schmidt condensation. The method is attractive as it selectively yields *E*-isomers. From the ^{1}H NMR spectra, all diaryl propenones were geometrically pure and with *trans* configuration (J = 15.50–15.60 Hz). Diaryl propenones were further cyclized to yield the tetrahydroquinolones by acid catalyzed deprotection of the acetylated amine to undergo simultaneous β-additions to the enone system. The 2-aryl tetrahydroquinolones showed a classical ABX system in the ^{1}H NMR and were further dehydrogenated to yield the dihydroquinolones employing molecular iodine. The dehydro-

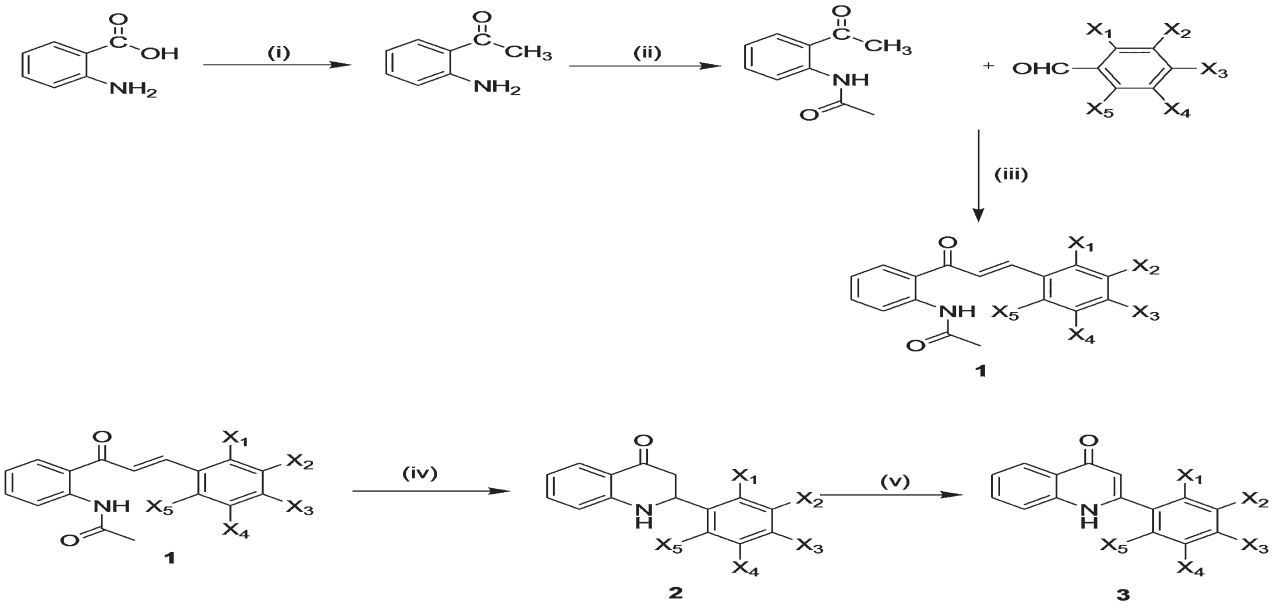

Scheme 1. Reagents and conditions: (i) CH_3Li/DME, aq NH_4Cl, stirring, 0°C, 1 h; (ii) $(CH_3CO)_2O$, C_6H_5N, MeOH, stirring, 70°C, 6 h; (iii) MeOH, 5% NaOH, stirring, rt, 6 h; (iv) EtOH, 5%HCl, reflux, 12 h; (v) DMSO, I_2, reflux, 12 h.

genated products were confirmed by the appearance of a singlet of the proton at 3 positions at 6.1–6.5 ppm. However in case of aryl rings (at the 2nd position) having oxygenated functionality at the *ortho* position, the signal for the proton at C-3 was found to be deshielded. The deshielded signal for the proton at C-3 can be attributed to intramolecular H bonding with the oxygen functionality at the *ortho* position of the 2-aryl ring. The dehydrogenation proceeded at C-2 and C-3. All the synthesized products (Table 1) were characterized by spectroscopic techniques.

Biological evaluation of the synthesized compounds for XO inhibitory activity

In vitro screening of the 2-aryl-4-quinolones (**3a**–**3o**) using bovine milk XO (grade 1, ammonium sulfate suspension) enzymatic assay was performed. Each synthesized compound was tested in triplicate for the XO inhibitory activity. Apigenin (earlier reported most active flavone) [19] and allopurinol were used as standards for the study. Among the series, compounds **3l**, **3k**, **3g** were found to be most active against XO with IC_{50} ranging from 6.24 to 12.0 μM (Table 2). The most active compound **3l** possessing the pyridinyl ring at the 2nd position exhibited significant inhibition (IC_{50} = 6.24 μM) in comparison to apigenin (IC_{50} = 10.21 μM) as well as allopurinol (IC_{50} = 8.31 μM). Compound **3k** with the thiophenyl ring also displayed significant inhibition with an IC_{50} = 11.23 μM followed by **3g** with 4-methoxy phenyl ring (IC_{50} = 12.02 μM).

The synthesis and biological evaluation of the series of compounds with diverse substitutions at the aryl ring (2nd position) such as halo, alkyl, alkoxy groups, and placement of bicyclic aryl/heteroaryl, cinnamyl, and heteroaryl at the 2nd position enabled us to correlate the dependence of the inhibitory activity of these molecules on the electronic and steric factors and thus a structure–activity relationship could be established. Careful investigation of Table 2 revealed interesting observations and indicated the influence of electronic and steric factors linked with the aryl ring at the 2nd position on the inhibitory potential of the molecules. In general, electronic factors such as introduction of deactivating groups, chloro and fluoro on the 2-phenyl ring resulted in a decrease in inhibitory activity as compared to the activating groups such as methoxy (compare **3h**, **3i** with **3b**, **3c**, **3d**, **3e**, **3g**, respectively). The presence of methoxy substituent and its position on the aryl ring played an important part in the inhibitory potential. Placement of a methoxy group on the aryl ring at the *para* position (**3g**) remarkably enhances the inhibitory activity. This can be attributed to the electron drift due to the methoxy group leading to quinoid formation (see Supporting Information) which enhances the rigidity of the molecules toward the planar structure. A methoxy group at the *ortho* position (**3d**) did not show any enhancement of the XO inhibitory activity and the activity profile was similar to the compound with unsubstituted phenyl ring (2nd position) (**3a**). The presence of an additional methoxy group apart from one

Table 1. % Yield and melting points of various products.

Compound	R_1	R_2	R_3	R_4	R_5	% Yield	mp (°C)
3a	H	H	H	H	H	75	250–252
3b	H	H	OCH_3	OCH_3	H	76	252–254
3c	OCH_3	OCH_3	H	H	H	78	233–235
3d	OCH_3	H	H	H	H	77	234–236
3e	OCH_3	H	H	OCH_3	H	76	260–262
3f	H	OCH_3	OCH_3	OCH_3	H	79	231–221
3g	H	H	OCH_3	H	H	75	288–290
3h	H	H	Cl	H	H	81	339–340
3i	H	H	F	H	H	80	250–252
3j			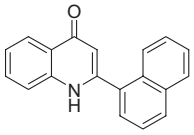			72	280–281
3k			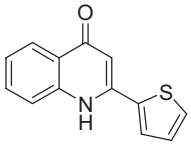			76	300–302
3l			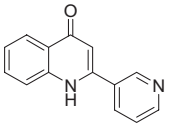			72	234–235
3m			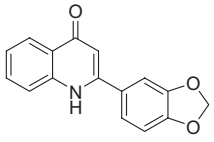			74	234–235
3n			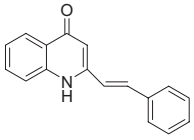			65	217–219
3o	H	H	CH_3	H	H	80	280–290

at the *para* position was not found to enhance the inhibitory activity (**3b**, **3f**). The placement of other activating groups such as methyl did not enhance the inhibitory activity which might be due to the absence of oxygen functionality and thus quinoid formation is not possible (**3o**). The presence of two oxygen functions (3rd and 4th position) at the phenyl ring (2nd position) forms *ortho* quinoid which does not contribute in bringing planarity of phenyl ring and thus no enhancement was observed on placing additional methoxy functionalities. A single methoxy group at the *ortho* position induces steric compression directing the molecule toward non-planarity. Apart from the electronic factors, steric factors also influenced the inhibitory activity such as change of the 2-phenyl ring with naphthyl (**3j**) leads to a drastic decrease in inhibitory potential which could be attributed to the steric bulk of the naphthyl. The steric bulk of naphthyl makes the molecule non-planar and planarity is a prerequisite for the inhibitory activity. Change of 2-phenyl with monocyclic heteroaryl rings such as thiophenyl (**3k**) and pyridinyl (**3l**) significantly enhanced the XO inhibitory

activity. The enhanced activity of **3k** and **3l** can be explained due to an increase in rigidity toward planar structure and by reducing the effect of rotamer formation through entirely different modes (see Supporting Information). Lengthening of the linker between the two rings (**3n**) led to the dilution of the XO inhibitory activity which could be due to the increase in the flexibility of the molecule and also indicates that increasing the distance between the two aryl rings (quinolone and the aryl) diminishes the activity.

Molecular modeling

The inhibition profile of synthesized 2-aryl-4-quinolones was investigated at the molecular level with the help of molecular docking. GOLD program was used to predict the binding pose of the potent XO inhibitor **3l** (Table 2), at the salicylic acid binding site of XO. The scoring function of the GOLD software was used to predict the strength of interaction between inhibitor (**3l**) and receptor. In each run, ten different conformations were generated out of which the conformation with the highest Gold score was selected for the study of ligand–receptor interaction. The salicylic acid binding cavity easily accommodates **3l** which shares hydrophobic, hydrogen bonding, and arene–arene interactions with the receptor. In the binding mode, the quinolone ring was found to be sandwiched in the hydrophobic pocket created by Leu873, Phe914, and Phe1009. **3l** forms two strong hydrogen bonds with binding residues, the first one is found between the hydroxyl group of Thr1010 with the carbonyl group of **3l** and another with the hydroxyl group of Glu802 with the nitrogen of **3l**. The pyridinyl ring fits in the hydrophobic cavity formed by Leu648, Leu1014, and Pro1076. Some energetically favorable arene–arene interactions were observed between **3l** and the receptor similar to salicylate in co-crystal of XO. The π-electrons of the quinolone ring were interacting with π-electrons of Phe914. The nitrogen lone pair of the pyridinyl is involved in van der Waals interactions with the residues in close proximity (Fig. 7a). A comparison study was done to get a clear vision of the binding mode of apigenin and the synthesized compound (**3l**) to rationalize their affinities for XO (Fig. 7b). Apigenin and **3l** show similar binding conformation in the binding site. In the salicylic acid binding site, apigenin get stabilized by the two hydroxyl groups attached to chromone ring which are involved in hydrogen bonding with Arg880, Phe914 and Glu1261. From the docking study, it can be deduced that the 2-aryl-4-quinolone molecule makes stronger interaction with the binding residues of XO because of additional hydrogen bonding between the –NH– in the quinolone ring of **3l** and Glu802. This additional hydrogen bond enhances the binding affinity for the inhibition of XO. The molecular modeling study concludes that our vision of isosteric replacement enhances the affinity for the XO enzyme due to the additional hydrogen bond between the quinoline ring and residues of XO.

Table 2. *In vitro* screening of the synthesized compounds (**3a–3o**) for XO inhibitory activity.

COMPOUNDS	XO inhibitory activity (IC_{50}, μM)
3a	18.0
3b	12.7
3c	12.5
3d	19.5
3e	18.2
3f	15.4
3g	12.0
3h	25.2
3i	26.3
3j	31.2
3k	11.23
3l	6.24
3m	30.8
3n	100
3o	18.3
Apigenin	10.21
Allopurinol	8.31

Conclusion

Bioisosterism has proved to be a useful lead optimization technique to improve the pharmacological activity, gain selectivity, and optimize the pharmacokinetics of the lead compounds. In continuation of our search for non-purine XO inhibitors, we designed 2-aryl-4-quinolones, also known as aza analogs of flavones as a new class of XO inhibitors. Aza analogs of flavones were designed after considerations of the pharmacophoric features and structural requisites for XO inhibition by one of the most privileged bioactive classes of secondary metabolites known as flavones. Thus the flavone framework was employed as the lead structure for further optimization. The design strategy involved isosteric replacement of chromone (a bicyclic unit present as a core structural unit in flavones) with quinolones after careful study of the enzyme's structural topography providing appropriate sites for interaction with the amino acid residues of the enzyme. On this basis, a series of 2-aryl/heteroaryl-4-quinolones was prepared and evaluated for *in vitro* XO inhibition. The results of the inhibitory evaluation indicated the strong influence of the electronic and steric factors linked with the aryl ring. The placement of heteroaryl rings proved to be critical for potentiating the inhibitory activity. SAR study revealed that: (i) the nature of the aryl ring, (ii) the nature of the substituent(s) on the aryl ring and (iii) the length of the linker greatly

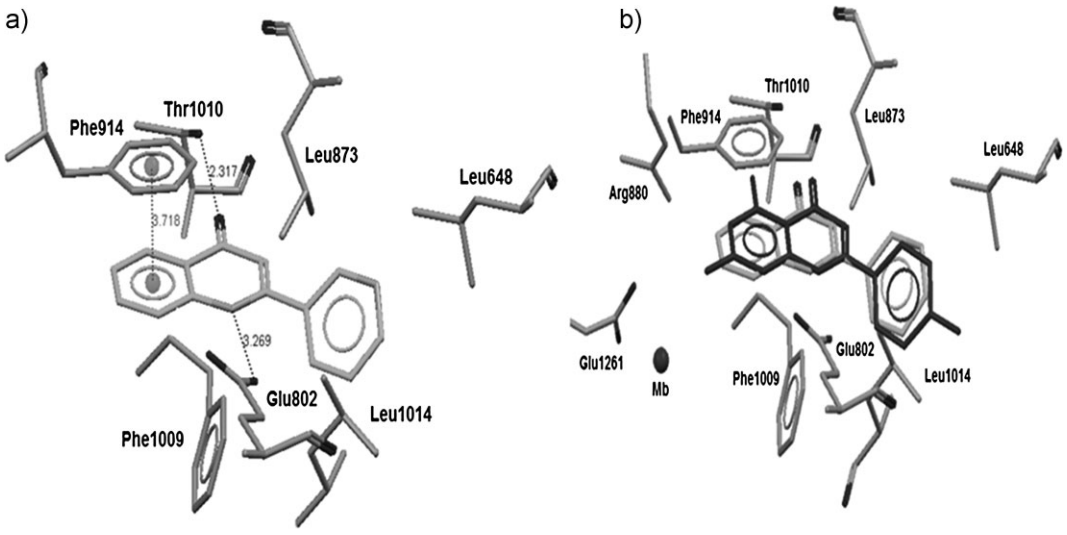

Figure 7. (a) Binding interactions of **3l** at the salicylic acid binding site of XO. (b) Superimposition of apigenin and **3l** at the salicylic acid binding site of XO.

affect the XO inhibitory activity. The factor enhancing the rigidity toward the planar structure remarkably enhanced the inhibitory activity and this feature is in agreement with the previously reported studies claiming the planarity to be an important structural feature for flavones. The results of the *in vitro assay* were further rationalized by molecular modeling studies. Docking simulations were performed to position the most active compound **3l** into the XO active site to determine the probable binding conformation, and the results confirmed that the compound was a potential inhibitor of XO. The docking studies further clarified the role of the heteroaryl ring responsible for the enhancement of the inhibition. The docking simulations also indicated that the bioisosteric replacement of chromones with quinolones in the design of aza analogs of flavones as non-purine based XO inhibitors preserves the key interactions with the enzyme and also provide some additional interaction sites. Rationalization of the *in vitro* inhibition results by the computational studies justified our design strategy. Further lead modification on **3l** such as synthesis of compounds with diverse permutation and combinations on ring A and B is under progress and will be published in due course.

Experimental

The reagents were purchased from Sigma–Aldrich, Loba and CDH, India, and used without further purification. All yields refer to isolated products after purification. Products were characterized by comparison with authentic samples and by spectroscopic data (IR, ^{1}H NMR). The spectra were measured in $CDCl_3$ and DMSO-d_6 relative to TMS (0.00 ppm). IR (KBr pellets) spectra were recorded on a Fourier transform infrared (FT-IR) Thermo spectrophotometer. Melting points were determined in open capillaries and were uncorrected.

Experimental procedure for the synthesis of 2-amino acetophenone

To a solution of 2-aminobenzoic acid (6.0 mmol) in DME (42 mL), methyl lithium (1.5 M in Et_2O, 13.2 mL, 19.8 mmol) was slowly added at 0°C. After being stirred for 1 h, the resulting solution containing white precipitates was quenched with saturated NH_4Cl (5 mL) and DME was evaporated under reduced pressure. The mixture was poured into saturated NH_4Cl (40 mL), extracted with methylene chloride (3 × 25 mL), and washed with saturated $NaHCO_3$ (40 mL). The combined organic phases were dried over $MgSO_4$, filtered, and concentrated under reduced pressure. The residues were purified by column chromatography to give 2-amino acetophenone.

Experimental procedure for the synthesis of *N*-(2-acetylphenyl)acetamide

A mixture of 2-amino acetophenone (0.1 mol, 13.5 g), 15 mL of acetic anhydride and a pinch of DMAP was stirred at 70°C in an oil bath for 6 h. The completion of reaction was monitored by TLC. The reaction mixture on completion was poured onto ice and the precipitates were collected and crystallized from ethanol.

Experimental procedure for the synthesis of diaryl propenones (1a–1o)

An aqueous solution of NaOH (5%, 4 mL) was added slowly to the stirring solution of appropriate aryl aldehyde (1 mmol) and *N*-(2-acetylphenyl)acetamide (1 mmol) in methanol (20 mL) in a 100 mL conical flask. The stirring was continued at room temperature for 6 h and the completion of reaction was moni-

tored by TLC. The reaction on completion was poured onto ice cold water; a yellow solid was obtained after filtration which was recrystallized from ethanol. The physical data for the characteristic compound is shown below.

*N-[2-(3-Phenylacryloyl)-phenyl]-acetamide (**1a**)*
Yield 77%; mp: 54–56°C (lit. 54–56°C) [27]; IR (KBr, cm^{-1}): 3321, 1660, 1652, 1590, 1240. ^1H NMR ($CDCl_3$, δ, TMS = 0): 8.71 (1H, d, J = 8.31 Hz), 7.98 (1H, d, J = 7.55 Hz), 7.86 (1H, d, J = 15.51 Hz), 7.65–7.38 (6H, m), 7.40 (1H, d, J = 15.51 Hz), 7.17 (1H, dd, J = 7.81 and 7.42 Hz), 2.26 (3H, s). Anal. calcd. for $C_{17}H_{15}NO_2$: C, 76.96; H, 5.70; N, 5.28. Found C, 77.21; H, 5.39; N, 5.34.

Experimental procedure for the synthesis of 2,3-dihydro-2-aryl quinolones (2a–2o)

A mixture of **1** (1 mmol) and 5% HCl (10 mL) was refluxed for 12 h. The reaction mixture was kept at room temperature and then basified with NH_4OH. The precipitated solid was filtered and recrystallized from ethanol. The physical data for the characteristic compound is shown below.

*2,3-Dihydro-2-phenylquinolin-4(1H)-one (**2a**)*
Yield 56%; mp: 149–150°C (lit. 150–151°C) [28]; IR (KBr, cm^{-1}): 3321, 1663, 1593, 1237. ^1H NMR ($CDCl_3$, 300 MHz, δ, TMS = 0): 7.87 (1H, dd, J = 8.10 and 1.51 Hz), 7.40–7.48 (4H, m), 7.31–7.35 (3H, m), 6.80 (1H, d, J = 8.11 Hz), 4.76 (1H, dd, J = 3.91 and 13.51 Hz), 4.49 (1H, s, NH, D_2O exchangeable proton), 2.90 (2H, dd, J = 13.50 and 16.21 Hz), 2.78 (2H, dd, J = 4.20 and 16.21 Hz). Anal. calcd. for $C_{15}H_{13}NO$: C, 80.69; H, 5.87; N, 6.27. Found C, 80.83; H, 5.64; N, 6.01.

Experimental procedure for the synthesis of 2-aryl-4-quinolones (3a–3o)

A mixture of **2** (1 mmol) and iodine (1.5 mmol) in DMSO was warmed at 80°C in an oil bath for 12 h. On completion of the reaction, the reaction mixture was poured onto a saturated solution of sodium thiosulfate. The precipitated solid was collected and the desired product was purified by column chromatography using silica gel (60 × 120 mesh) with increasing percentage of ethyl acetate in hexane as eluting solvent. The physical data of the compounds are provided below.

*2-Phenylquinolin-4(1H)-one (**3a**)*
mp: 250–252°C (lit. 252–254°C) [28]. IR (KBr, cm^{-1}): 3321, 2978, 1666, 1591, 1233. ^1H NMR (DMSO-d_6, 300 MHz, δ, TMS = 0): 11.45 (1H, s), 8.29 (1H, d, J = 8.41 Hz), 7.62–7.77 (5H, m), 7.60–7.62 (2H, m), 7.32 (1H, t, J = 8.11 Hz), 6.48 (1H, s). Anal. calcd. for $C_{15}H_{11}NO$: C, 81.43; H, 5.01; N, 6.33. Found: C, 81.66; H, 4.99; N, 6.64.

*2-(3,4-Dimethoxyphenyl)-quinolin-4(1H)-one (**3b**)*
mp: 252–254°C. IR (KBr, cm^{-1}): 3328, 2972, 1665, 1594, 1313, 1237. ^1H NMR (DMSO-d_6, 300 MHz, δ, TMS = 0): 8.11 (1H, d, J = 7.21 Hz), 7.75 (1H, d, J = 8.40 Hz), 7.64 (1H, m), 7.31 (1H, m), 7.01–7.06 (3H, m), 6.41 (1H, s), 3.92 (6H, s). Anal. calcd. for $C_{17}H_{15}NO_3$: C, 72.58; H, 5.37; N, 4.98. Found: C, 72.66; H, 5.48; N, 4.78.

*2-(2,3-Dimethoxyphenyl)quinolin-4(1H)-one (**3c**)*
mp: 233–235°C. IR (KBr, cm^{-1}): 3333, 2975, 1669, 1597, 1309, 1232. ^1H NMR (DMSO-d_6, 300 MHz, δ, TMS = 0): 8.20 (1H, d, J = 8.7 Hz), 8.11 (1H, d, J = 7.5 Hz), 7.78 (1H, m), 7.26–7.28 (3H, m), 7.17 (2H, m), 3.95 (3H, s), 3.80 (3H, s). Anal. calcd. for $C_{17}H_{15}NO_3$: C, 72.58; H, 5.37; N, 4.98. Found: C, 72.34; H, 5.22; N, 5.11.

*2-(2-Methoxyphenyl)-quinolin-4(1H)-one (**3d**)*
mp: 234–236°C (lit. 233–235°C) [29]. IR (KBr, cm^{-1}): 3341, 2969, 1663, 1596, 1311, 1229. ^1H NMR (DMSO-d_6, 400 MHz, δ, TMS = 0): 8.34–8.36 (1H, m), 8.03–8.07 (1H, m), 7.76–7.80 (1H, m), 7.67–7.71 (2H, m), 7.35 (1H, m), 7.29 (1H, s), 7.26 (1H, m), 3.90 (3H, s). Anal. calcd. for $C_{16}H_{13}NO_2$: C, 76.48; H, 5.21; N, 5.57. Found: C, 76.14; H, 5.12; N, 5.77.

*2-(2,5-Dimethoxyphenyl)-quinolin-4(1H)-one (**3e**)*
mp: 260–262°C. IR (KBr, cm^{-1}): 3329, 2981, 1659, 1588, 1303, 1224. ^1H NMR (DMSO-d_6, 300 MHz, δ, TMS = 0): 8.09 (2H, m), 7.83 (1H, d, J = 8.70 Hz), 7.18–7.33 (4H, m), 7.02 (1H, s), 3.85 (6H, s). Anal. calcd. for $C_{17}H_{15}NO_3$: C, 72.58; H, 5.37; N, 4.98. Found: C, 72.74; H, 5.43; N, 4.77.

*2-(3,4,5-Trimethoxyphenyl)-quinolin-4(1H)-one (**3f**)*
mp: 231–221°C (lit. 232–234°C) [30]. IR (KBr, cm^{-1}): 3335, 2973, 1664, 1585, 1305, 1222. ^1H NMR (DMSO-d_6, 300 MHz, δ, TMS = 0): 8.11 (1H, d, J = 7.21), 7.75 (1H, d, J = 8.40 Hz), 7.64 (1H, m), 7.31 (1H, m), 7.08 (2H, s), 6.41 (1H, s), 3.92 (9H, s). Anal. calcd. for $C_{18}H_{17}NO_4$: C, 69.44; H, 5.50; N, 4.50. Found: C, 69.64; H, 5.53; N, 4.37.

*2-(4-Methoxyphenyl)-quinolin-4(1H)-one (**3g**)*
mp: 287–288°C (lit. 288–290°C) [28]. IR (KBr, cm^{-1}): 3329, 2978, 1662, 1587, 1306, 1225. ^1H NMR (DMSO-d_6, 300 MHz, δ, TMS = 0): 11.37 (1H, s), 8.27 (1H, d, J = 7.21 Hz), 7.72 (3H, m), 7.59 (1H, t, J = 8.10 Hz), 7.31(1H, t, J = 7.51 Hz), 7.04 (1H, d, J = 8.70 Hz), 6.45 (1H, s). Anal. calcd. for $C_{16}H_{13}NO_2$: C, 76.48; H, 5.21; N, 5.57. Found: C, 76.84; H, 5.32; N, 5.26.

*2-(4-Chlorophenyl)-quinolin-4(1H)-one (**3h**)*
mp: 339–340°C (lit. 340–342°C) [28]. IR (KBr, cm^{-1}): 3343, 2971, 1665, 1586, 1222, 751. ^1H NMR (DMSO-d_6, 300 MHz, δ, TMS = 0): 11.77 (1H, s), 8.11 (2H, dd, J = 8.11 and 1.20 Hz), 7.88 (2H, d, J = 2.80 Hz), 7.76 (1H, J = 8.12 Hz), 7.68–7.71 (1H, m), 7.66 (2H, d, J = 8.61 Hz), 7.33–7.38 (1H, m), 6.38 (1H, s). Anal. calcd. for $C_{15}H_{10}ClNO$: C, 70.46; H, 3.94; Cl, 13.87; N, 5.48. Found: C, 70.24; H, 3.62; Cl, 13.99; N, 5.16.

*2-(4-Fluorophenyl)-quinolin-4(1H)-one (**3i**)*
mp: 250–252°C. IR (KBr, cm^{-1}): 3339, 2966, 1662, 1583, 1228, 911. ^1H NMR (DMSO-d_6, 300 MHz, δ, TMS = 0): 8.09 (1H, d, J = 7.60 Hz), 7.91 (2H, m), 7.75 (1H, d, J = 8.42 Hz), 7.67 (1H, t, J = 7.62 Hz), 7.43 (2H, m), 7.33 (1H, t, J = 7.21 Hz), 6.34 (1H, s). Anal. calcd. for $C_{15}H_{10}FNO$: C, 75.30; H, 4.21; F, 7.94; N, 5.85. Found: C, 75.49; H, 4.52; Cl, 7.79; N, 5.46.

*2-(Naphthalen-1-yl)-quinolin-4(1H)-one (**3j**)*
mp: 280–281°C (lit. 284–285°C) [30]. IR (KBr, cm^{-1}): 3344, 2972, 1660, 1585, 1230. ^1H NMR (DMSO-d_6, 300 MHz, δ, TMS = 0): 12.01 (1H, s), 8.20 (2H, m), 8.03–8.11 (3H, m), 7.89 (1H, d, J = 6.90 Hz), 7.55–7.70 (4H, m), 7.33 (1H, m), 6.20 (1H, s). Anal. calcd.

for $C_{19}H_{13}NO$: C, 84.11; H, 4.83; N, 5.16. Found: C, 84.44; H, 4.42; N, 5.36.

*2-(Thiophen-2-yl)quinolin-4(1H)-one (**3k**)*

mp: 300–302°C (lit. 300°C) [29]. IR (KBr, cm^{-1}): 3343, 2985, 1659, 1577, 1313, 1225. ^{1}H NMR (DMSO-d_6, 300 MHz, δ, TMS = 0): 8.10 (1H, d, J = 8.80 Hz), 8.05 (1H, s), 7.70 (1H, d, J = 6.40 Hz), 7.54 (1H, t, J = 8.00 Hz), 7.32 (1H, m), 6.87 (1H, s), 6.55 (1H, s), 6.37 (1H, s). Anal. calcd. for $C_{13}H_9NO_2$: C, 73.92; H, 4.29; N, 6.63. Found: C, 73.74; H, 4.52; N, 6.96.

*2-(Pyridin-4-yl)-quinolin-4(1H)-one (**3l**)*

mp: 234–235°C. IR (KBr, cm^{-1}): 3335, 2977, 1658, 1583, 1233. ^{1}H NMR (DMSO-d_6, 300 MHz, δ, TMS = 0): 12.19 (1H, s), 9.05 (1H, s), 8.69 (1H, m), 8.34 (1H, d, J = 7.2 Hz), 8.24 (1H, m), 7.70 (2H, m), 7.62 (1H, m), 7.45 (1H, m). Anal. calcd. for $C_{14}H_{10}N_2O$: C, 75.66; H, 4.54; N, 12.60. Found: C, 75.44; H, 4.82; N, 12.46.

*2-(3,4-Methylenedioxyphenyl)-1,4-dihydro-4-oxoquinoline (**3m**)*

mp: 234–235°C (lit. 284–285°C) [30]. IR (KBr, cm^{-1}): 3464, 1636, 2981, 1580, 1315, 1221. ^{1}H NMR (DMSO-d_6, 300 MHz, δ, TMS = 0): 8.09 (1H, dd, J = 1.35, 8.30 Hz), 7.77 (1H, d, J = 8.30 Hz), 7.76 (1H, d, J = 8.30 Hz), 7.63 (1H, m), 7.23–7.45 (3H, m), 7.08 (1H, d, J = 8.30 Hz), 6.37 (1H, s), 6.12 (2H, s). Anal. calcd. for $C_{16}H_{11}NO_3$: C, 72.45; H, 4.18; N, 5.28. Found: C, 72.64; H, 4.42; N, 5.06.

*2-Styrylquinolin-4(1H)-one (**3n**)*

mp: 217–219°C. IR (KBr, cm^{-1}): 3440, 1644, 2977, 1565, 1239. ^{1}H NMR (DMSO-d_6, 400 MHz, δ, TMS = 0): 11.73 (1H, s), 8.05 (1H, d, J = 8.00 Hz), 7.63–7.75 (5H, m), 7.44–7.47 (2H, m), 7.39 (1H, m), 7.30 (1H, t, J = 7.20 Hz), 7.18 (1H, d, J = 16.4 Hz), 6.37 (1H, s). Anal. calcd. for $C_{17}H_{13}NO$: C, 82.57; H, 5.30; N, 5.66. Found: C, 82.69; H, 5.48; N, 5.36.

*2-(4-Methylphenyl)-4-quinolone (**3o**)*

mp: 286–287°C (lit. 288–290°C) [28]. IR (KBr, cm^{-1}): 3440, 1644, 2977, 1565, 1239. ^{1}H NMR (DMSO-d_6, 300 MHz, δ, TMS = 0): 11.69 (1H, s), 8.10 (1H, dd, J = 8.1 Hz and 1.2 Hz), 7.69–7.79 (3H, m), 7.63–7.67 (1H, m), 7.31–7.41 (3H, m), 6.34 (1H, s), 2.33 (3H, s). Anal. calcd. for $C_{16}H_{13}NO$: C, 81.68; H, 5.57; N, 5.95. Found: C, 81.39; H, 5.24; N, 6.19.

XO assay

Bovine milk XO (grade 1, ammonium sulfate suspension; Sigma–Aldrich) activity was assayed spectrophotometrically by measuring the uric acid formation at 293 nm using a Hitachi U-3010 UV–Visible spectrophotometer at 25°C [31]. The reaction mixture contained 50 mM potassium phosphate buffer (pH 7.6), 75 μM xanthine, and 0.08 units of XO. Inhibition of XO activity by various inhibitors was measured by following the decrease in the uric acid formation at 293 nm at 25°C. The enzyme was preincubated for 5 min with the test compound dissolved in DMSO (1% v/v), and the reaction was started by the addition of xanthine. Final concentration of DMSO (1% v/v) did not interfere with the enzyme activity. All the experiments were performed in triplicate and values were expressed as means of three experiments.

Molecular modeling

A flexible docking study of the most active compound at the salicylic acid binding site of XO was performed with the help of GOLD software [32]. To validate the docking procedure for the prediction of the correct binding mode of the inhibitor at the salicylic acid binding site, the salicylic acid was extracted from the original X-ray structure (1FIQ) [33] and re-docked using GOLD [32]. The highest scoring conformation was selected and compared with the X-ray structure conformation. The docked conformation of salicylic acid was found to be similar to the original X-ray structure conformation. The root mean square deviation (RMSD) between the best scored conformers from docking and X-ray structure was found to be 0.21 Å.

Special thanks to Dr. K. A. Suri, Ex-Director Grade Scientist, IIIM (CSIR), Jammu, for providing pure sample of apigenin.

The authors have declared no conflict of interest.

References

[1] S. L. Stockert, S. S. Shinde, R. F. Anderson, R. J. Hille, *J. Am. Chem. Soc.* **2002**, *124*, 554–555.

[2] F. Borges, E. Fernandes, F. Roleira, *Curr. Med. Chem.* **2002**, *9*, 195–217.

[3] R. Hille, *Eur. J. Inorg. Chem.* **2006**, *10*, 1913–1926.

[4] P. Pacher, A. Nivorozhkin, C. Szabo, *Phamacol. Rev.* **2006**, *58*, 87–114.

[5] (a) G. B. Elion, S. Callahan, H. Nathan, S. Bieber, R. W. Rundles, G. H. Hitching, *Biochem. Pharmacol.* **1963**, *12*, 85–93; (b) H. Tamta, R. Thilagavathi, A. K. Chakraborti, A. K. Mukhopadhyay, *J. Enzyme Inhib. Med. Chem.* **2005**, *20*, 317–324.

[6] R. K. Robins, G. R. Revankar, D. E. Brien, R. H. Springer, T. N. A. Albert, K. Senga, J. P. Miller, D. G. J. Streeter, *J. Heterocycl. Chem.* **1985**, *22*, 601–634.

[7] K. Oettl, G. Reibneggar, *Biochim. Biophys. Acta* **1999**, *1430*, 387–395.

[8] (a) J. J. Baldwin, P. A. Kasinger, F. C. Novello, J. M. Sprague, D. E. Duggan, *J. Med. Chem.* **1975**, *18*, 895–900; (b) J. J. Baldwin, P. K. Lumma, F. C. Novello, G. S. Ponticello, J. M. Sprague, D. E. J. Duggan, *J. Med. Chem.* **1977**, *20*, 1189–1191; (c) Y. Osada, M. Tsuchimoto, H. Fukushima, K. Takahashi, S. Kondo, M. Hasegawa, K. Komoriya, *Eur. J. Pharmacol.* **1993**, *241*, 183–188.

[9] K. Okamoto, B. T. Eger, T. Nishino, S. Kondo, E. F. Pai, T. Nishino, *J. Biol. Chem.* **2003**, *278*, 1848–1855.

[10] (a) P. Cos, L. Ying, M. Calomme, J. P. Hu, K. Cimanga, B. V. Poel, L. Pieters, A. Vlietincka, D. V. Berghe, *J. Nat. Prod.* **1998**, *61*, 71–76; (b) D. E. Van-Hoorn, R. J. Xijveidt, P. A. Van-Leeuwen, Z. Hofman, L. Rabet, D. B. De-Bont, K. Van-Norren, *Eur. J. Pharmacol.* **2002**, *451*, 111–118.

[11] K. Okamoto, K. Matsumoto, R. Hille, B. T. Eger, E. F. Pai, T. Nishino, *Proc. Natl. Acad. Sci. USA* **2004**, *101*, 7931–7936.

[12] L. Shen, H. F. Ji, *Bioorg. Med. Chem. Lett.* **2009**, *19*, 5990–5993.

[13] K. Nepali, G. Singh, A. Turan, A. Agarwal, S. Sapra, R. Kumar, U. C. Banerjee, P. K. Verma, N. K. Satti, M. K. Gupta, O. P. Suri, K. L. Dhar, *Bioorg. Med. Chem.* **2011**, *19*, 1950–1958.

[14] K. Nepali, A. Agarwal, S. Sapra, V. Mittal, R. Kumar, U. C. Banerjee, M. K. Gupta, N. K. Satti, O. P. Suri, K. L. Dhar, *Bioorg. Med. Chem.* **2011**, *19*, 5569–5576.

[15] J. Bostrom, K. Berggren, T. Elebring, P. J. Greasley, M. Wilstermann, *Bioorg. Med. Chem.* **2007**, *15*, 4077–4084.

[16] W. Plummer, P. E. Finke, S. G. Mills, J. Wang, X. Tong, G. A. Doss, T. M. Fong, J. Z. Lao, M. T. Schaeffer, J. Chen, C. P. Shen, D. S. Stribling, L. P. Shearman, A. M. Strack, L. H. T. Van-der Ploeg, *Bioorg. Med. Chem. Lett.* **2005**, *15*, 1441–1446.

[17] J. H. Lange, H. H. Van-Stuivenberg, H. K. A. C. Coolen, T. J. P. Adolfs, A. C. McCreary, H. G. Keizer, H. C. Wals, W. Veerman, A. J. M. Borst, W. De-Looff, P. C. Verveer, C. G. Kruse, *J. Med. Chem.* **2005**, *48*, 1823–1838.

[18] J. H. M. Lange, C. G. Kruse, H. H. Van-Stuivenberg, U. S. Patent 05/0171179, **2005** [*Chem. Abstr.* 2005, 143, 172869].

[19] S. Mills, K. Bone, *Principles and Practice of Phytotherapy*, Churchill Livingstone, New York **2000**, p. 31.

[20] E. Middleton, Jr, K. Chithan, The impact of plant flavonoids on mammalian biology: implications for immunity, inflammation and cancer, in *The Flavonoids: Advances in Research Since 1986* (Ed.: J. B. Harborne), Chapman and Hall, London, UK **1993**.

[21] S. P. Fernandez, C. Wasowski, L. M. Loscalzo, R. E. Granger, G. A. R. Johnston, A. C. Paladini, M. Marder, *Eur. J. Pharmacol.* **2006**, *539*, 168–176.

[22] J. B. Harborne, C. A. Williams, *Phytochemistry* **2000**, *55*, 481.

[23] P. Cos, L. Ying, M. Calomme, J. P. Hu, K. Cimanga, B. Van-Poel, L. Pieters, A. J. Vlietinck, D. V. Berghe, *J. Nat. Prod.* **1998**, *61*, 71–76.

[24] S. L. Da-Silva, A. Da-Silva, K. M. Honorio, S. Marangoni, M. H. Toyama, A. B. F. Da-Silva, *J. Mol. Struct. Theochem.* **2004**, *684*, 1–8.

[25] M. Lin, C. S. Chen, C. T. Chen, Y. C. Liang, J. K. Lin, *Biochem. Biophys. Res. Commun.* **2002**, *294*, 167–169.

[26] A. Ahmeda, M. Daneshtalaba, *J. Pharm. Pharm. Sci.* **2012**, *15*, 52–72.

[27] S. Sharma, S. Kumar, K. Nepali, S. Sapra, O. P. Suri, K. L. Dhar, G. S. Sarma, A. K. Saxena, *Indian J. Pharm. Sci.* **2010**, *72*, 801–806.

[28] J. I. Lee, J. S. Youn, *Bull. Korean Chem. Soc.* **2008**, *29*, 1853–1856.

[29] D. Ding, X. Li, X. Wang, Y. Du, J. Shen, *Tetrahedron Lett.* **2006**, *47*, 6997–6999.

[30] S. Torii, H. Okumoto, L. H. Xu, M. Sadakane, M. V. Shostakovsky, A. B. Ponomaryov, V. N. Kalinin, *Tetrahedron* **1993**, *49*, 6773–6784.

[31] (a) J. Escribano, F. Gracia-Canovas, *Biochem. J.* **1988**, *254*, 829–833; (b) Y. Takano, K. Hase-Aoki, H. Horiuchi, L. Zhao, Y. Kasahara, S. Kondo, M. A. Becker, *Life Sci.* **2005**, *76*, 1835–1847.

[32] GOLD, Evaluation Version 4.0.1. Cambridge Crystallographic Data Centre, Cambridge, UK **2009**.

[33] C. Enroth, B. T. Eger, K. Okamoto, T. Nishino, E. F. Pai, *Proc. Natl. Acad. Sci. USA* **2000**, *97*, 10723–10727.

